Electron paramagnetic resonance response and magnetic interactions in ordered solid solutions of lithium nickel oxides

1996 J. Phys.: Condens. Matter 8 7339

(http://iopscience.iop.org/0953-8984/8/39/010)

J. Phys.: Condens. Matter **8** (1996) 7339–7347. Printed in the UK

Electron paramagnetic resonance response and magnetic interactions in ordered solid solutions of lithium nickel oxides

C B Azzoni†, A Paleari‡, V Massarotti§ and D Capsoni§

† Istituto Nazionale di Fisica della Materia, Dipartimento di Fisica 'Alessandro Volta', Universitá di Pavia, via Bassi 6, I-27100 Pavia, Italy

‡ Istituto Nazionale di Fisica della Materia, Dipartimento di Fisica, Universitá di Milano, via Celoria 16, I-20133 Milano, Italy

§ Dipartimento di Chimica-Fisica, Universitá di Pavia, via Taramelli 16, I-27100 Pavia, Italy

Received 2 April 1996, in final form 23 May 1996

Abstract. EPR data of ordered solid solutions of lithium nickel oxides are reported as a function of the lithium content. The features of the signal and the EPR centre density are analysed by a model of dynamical trapping of holes in [Ni^{2+}–O–Ni^{2+})–h^+] complexes. The possible origin of the interactions responsible for the magnetic ordering and some features of the transport properties are also discussed.

1. Introduction

Mixed lithium nickel oxides may show a variety of magnetic features. In fact, the magnetic order depends on the lithium content and on the preparation method [1] and may be reminiscent of the magnetic properties of one of the two borderline structural phases: the cubic NiO and the $LiNiO_2$ layered compound.

$Li_xNi_{1-x}O$ solid solutions, with $x < 0.3$, are substitutional solid solutions (SSSs) with cubic NaCl structure and magnetic properties deriving from the dilution of the antiferromagnetic (AF) NiO [1–3]. Compounds with $x > 0.3$ consist of ordered solid solutions (OSSs), usually indicated as $Li_{2x}Ni_{2-2x}O_2$ [4], with a rhombohedral cell and two distinct cationic sites. Except for the quasi-stoichiometric compounds ($x > 0.46$) [5–7], the OSS phases show ferrimagnetic transitions. Ferrimagnetic ordering was interpreted as arising from AF interactions between 'heavy' cationic layers, containing Ni^{2+} and Ni^{3+} ions, and 'light' layers of Li^+ and Ni^{2+} ions [1, 8]. According to this approach, the electronic holes introduced by lithium substitution of nickel ions are localized in nickel sites of 'heavy' layers. An alternative viewpoint relates the magnetic ordering to interactions between Ni^{2+} d electrons and oxygen 2p holes [9]. Indeed the kind of hole localization in lithium-substituted nickel oxides is still a matter of debate. X-ray absorption [9, 10], nuclear magnetic resonance (NMR) [3, 5] and electron paramagnetic resonance (EPR) [1, 5, 8, 11–14] studies have already been carried out to investigate this aspect, but a clear-cut picture was not achieved. For example, different opinions still exist about the interpretation of the EPR response.

The first goal of this work was to reconsider the EPR spectrum observed in OSS compounds in order to clarify its origin. To do this, a careful analysis of the density of

0953-8984/96/397339+09$19.50

paramagnetic centres was carried out and the EPR responses resulting from the possible coordination geometries were evaluated. The thermal behaviour of the signal lineshape was also considered as well as the asymmetry of the signal observed just above the magnetic transition temperature T_c. Finally, the possible exchange interactions were discussed and related to the long-range magnetic ordering.

2. Samples and measurements

Pure OSS compounds were prepared from the reactive system NiO–Li_2CO_3 by starting with a lithium cationic fraction $x \simeq 0.5$. The reagents were mixed and heated at $5\,^{\circ}C\ min^{-1}$ up to $800\,^{\circ}C$ in alumina and then cooled at $5\,^{\circ}C\ min^{-1}$ to room temperature. Samples with different lithium contents were obtained after different annealing times by Li_2O evaporation during the high-temperature isothermal step [1]. The sample composition and structural parameters of the OSS phase were controlled by x-ray diffraction (XRD) measurements obtained with a Philips PW 1710 powder diffractometer [1]. In table 1 we report the compositions deduced from XRD data.

Table 1. Composition of $Li_{2x}Ni_{2-2x}O_2$ samples. For each x-value of lithium addition the magnetic transition temperature T_c from static magnetic susceptibility measurements [1] is reported, together with the slope $d(\Delta B)/dT$, computed from room temperature down to just above T_c; in this range, ΔB is linear with T.

x	T_c (K)	$d(\Delta B)/dT$ (mT K^{-1})
0.461	105	0.64
0.416	214	1.45
0.399	214	1.44
0.359	241	2.00
0.348	252	2.20

EPR measurements were carried out at 9.12 GHz in the temperature range 120–300 K using a Bruker spectrometer. Care was taken to achieve a reproducible sample position in the resonant cavity for correct signal comparison. Appropriate amounts of sample (a few milligrams) were employed to keep constant the Q-factor of the resonant cavity. The spectra were analysed by numerical methods which allowed the double integration of the signals. The experimental spectra were compared with calculated spectra obtained by parameters deduced from the crystal-field analysis. Absolute values of paramagnetic centre density were estimated using an *ad hoc* paramagnetic standard consisting of a Li_2MnO_3 powder sample, prepared and tested for that purpose; the EPR signal of this compound is characterized by a constant lineshape (Lorentzian symmetric) throughout the investigated temperature range and by a linewidth and an intensity comparable with those of the observed signals. The calculated spin density values range between 10^{21} and $7 \times 10^{21}\ cm^{-3}$.

3. Results and discussion

3.1. Electron paramagnetic resonance signal

The investigated samples, irrespective of their compositions, show at 300 K similar EPR spectra, consisting of one symmetric signal with $g \simeq 2.139$ (figure 1, curve (A)). Previously

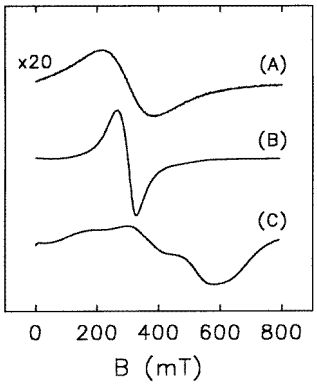

Figure 1. EPR signals of $Li_{0.8}Ni_{1.2}O_2$ at different temperatures: curve (A), $T = 290$ K; curve (B), $T = 200$ K; curve (C), $T = 150$ K.

reported EPR data for a wide range of compositions [1], comprising both OSS and SSS compounds, support the association of this signal with the OSS phase, no signal arising from the SSS phase.

From 300 K down to just above the magnetic transition, the EPR spectra are characterized by signal narrowing and the linewidth ΔB shows a linear behaviour with the temperature whose slope $d(\Delta B)/dT$ is sample dependent. ΔB reaches a minimum at a temperature matching well the magnetic transition temperature T_c deduced from static susceptibility measurements [1] (table 1). Just above T_c, the lineshape becomes asymmetric (figure 1, curve (B)). Below T_c, the EPR signal broadens and finally splits into more components (figure 1, curve (C)) whose resonance fields and linewidths show sample-dependent behaviours.

Similar EPR spectral features were reported by other workers; both low-spin (LS) Ni^{3+} ($S = 1/2$) [5, 8, 11, 12] and high-spin (HS) Ni^{3+} ($S = 3/2$) assignments [13, 14] were proposed. Indeed the attribution of the observed signal to the HS Ni^{3+} ion should be ruled out, because a strongly anisotropic spectrum is expected in this case [13]. Anyway, all the EPR studies demonstrated the d character of the holes. Nevertheless, our data suggest that the EPR centre density and the expected concentration of Ni^{3+} ions (proportional to $2x$) are not simply related, as shown in figure 2.

In order to interpret this experimental evidence and to clarify the origin of the EPR signal we have to reconsider the distribution and dynamics of the electronic holes.

3.2. Hole dynamics

Nickel ions facing lithium ions in adjacent cationic layers constitute the peculiar structural feature of $LiNiO_2$. This structure, compared with that of NiO, involves the substitution of Ni^{2+} by Li^+ ions, compensated by an equal amount of electronic holes. In quasi-stoichiometric samples, conductivity measurements showed the presence of electronic holes with a relatively low activation energy (about 0.2 eV) [15]. These holes should be partially delocalized and one might be tempted to attribute the observed EPR spectrum to the superposition of signals from Ni^{2+} ions and holes rather than to Ni^{3+} sites. However, highly efficient broadening processes should be active in this case, as has already been suggested to explain the lack of EPR signal in the SSS phases [1, 3], making the presence of a detectable EPR signal unlikely.

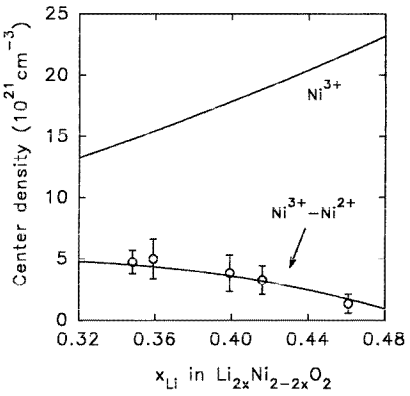

Figure 2. EPR centre density versus lithium content x compared with the calculated density of Ni^{3+} ions and of nickel pairs facing on adjacent cationic layers.

Thus, the EPR signal observed in non-stoichiometric compounds probably arises from other mechanisms. Indication of the nature of the EPR centres may be derived from structural arguments. In fact we remark that in $Li_{2x}Ni_{2-2x}O_2$ compounds with $x < 0.5$ a fraction $1-2x$ of nickel ions is also found in the Li-rich 'light' layers, forming Ni–O–Ni sites with the nickel ions of 'heavy' layers. These sites should behave as hole traps owing to their singular geometry with respect to the standard Ni–O–Li sites of the $LiNiO_2$ parent compound. If some sort of hole localization takes place in these sites, the resulting [(Ni^{2+}–O–Ni^{2+})–h^+] complexes might be responsible for the EPR signal. In support of this, we found good agreement (see figure 2) between the dependence of the EPR centre density on the lithium content and the statistical occurrence of the pairs of nickel ions facing each other on opposite sides of oxygen layers (proportional to $2x(1-2x)$).

These localized holes should possess a partial d character, as suggested by the high g-value of the EPR signal and also supported by recent NMR results [5]. So, we may suppose that these holes dwell on the nickel sites, but in a dynamic trapping situation between the nickel ions bridged by the oxygen. In this approach, holes transitorily trapped on Ni^{2+} ions give rise to Ni^{3+} ions. Thus, the symmetric EPR spectrum at $T > T_c$ would consist of the time average of signals arising from the Ni^{2+} and Ni^{3+} ions sharing the hole. In order to define this picture better we shall try to clarify the symmetry features that one may expect in the [Ni^{2+}–O–Ni^{2+})–h^+] complex.

3.3. Local structure

From the refinement of the XRD data [4], the Ni–O mean distance (0.198 nm) pertaining to the nickel ions of the 'heavy' layers differs from that (0.211 nm) of the ions in the 'light' layers. Consistently, the oxygen octahedra around the nickel ions of the 'heavy' ('light') layers are trigonally compressed (elongated) along the c axis. The resulting mean angle between two facing cations is about 175° (figure 3(A)).

Nevertheless, the real local configuration of the [(Ni^{2+}–O–Ni^{2+})–h^+] complex should be different from the mean geometry considered above, more appropriate to the Ni–O–Li sites, and should probably approach the Ni–O–Ni environment in NiO (figure 3(B)). So, local rearrangements of the anionic positions might align the axes of the two octahedra along the Ni–O–Ni direction (the fourfold octahedral axis) to obtain two nearly regular

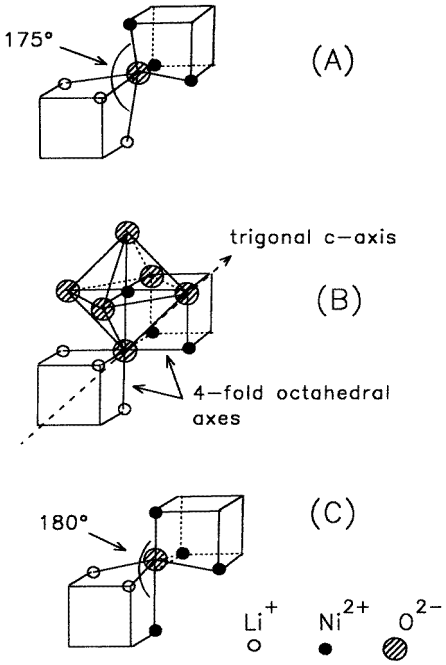

Figure 3. (A) OSS structure with trigonal distortions; (B) sketch of the oxygen coordination in the idealized NiO structure; (C) rearrangement of the atomic positions around the Ni–O–Ni complex according to the present model (see text). In (A) and (C) the angles and bond distortions are exaggerated.

octahedra with a small tetragonal distortion (estimated to be a factor of about 10^{-3} smaller than the Ni–O distance): a contracted octahedron and an elongated octahedron around the nickel ions in 'heavy' and 'light', layers respectively (figure 3(C)).

This local geometry allows a strong overlap between d orbitals and anionic ligand orbitals. The resulting increase in covalency should enhance the crystal field (CF) around the Ni^{2+} ions where the holes are trapped, stabilizing the LS state of Ni^{3+} ions. In fact, pure CF calculations give an energy splitting of about 0.5 eV, clearly too small if compared with the gain of Coulomb energy between LS and HS configurations which we estimate to be 16B ($\simeq$2 eV), where $B \simeq 10^3$ cm^{-1} is the Racah parameter.

Ni^{2+} $3d^8$ ions ($L = 3$, $S = 1$) in environments of this type give nearly symmetric signals with $g \geqslant 2$ owing to the very small distortion [16]. On the other hand, the unpaired electron of Ni^{3+} $3d^7$ ions (LS configuration with $S = 1/2$) in the contracted octahedra is in a $|x^2 - y^2\rangle$-like state giving $2 \simeq g_\perp < g_\parallel$ while, in the elongated octahedra, it is in a $|3z^2 - r^2\rangle$-like state giving $g_\perp > g_\parallel \simeq 2$. So, we note that the different Ni^{3+} sites are characterized by opposite anisotropies. Therefore, if the hole is dynamically shared between the nickel ions, we expect that the resulting average EPR signal may be nearly symmetric with $g > 2$ if the linewidth of the single signals is large enough compared with their g anisotropies. Indeed, the g-values calculated by CF methods from the oxygen coordinations obtained by structural data are in good agreement with the experiment. In fact, for Ni^{2+} we calculated $g = 2.138$, for LS Ni^{3+} in the contracted octahedra the estimated values are $g_\perp = 2.06$ and $g_\parallel = 2.35$ while, in the elongated octahedra, $g_\perp = 2.15$ and $g_\parallel = 2.00$. The calculated powder signal, resulting from the superposition of these signals (taking a

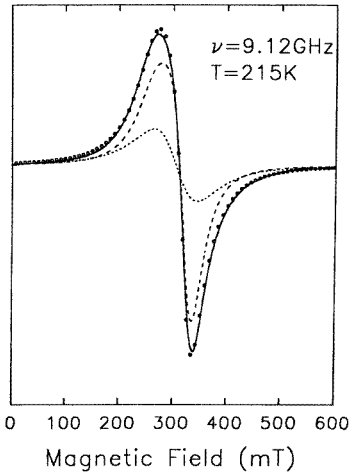

Figure 4. Numerical simulations (○) of the asymmetric EPR signal (——) of $Li_{0.8}Ni_{1.2}O_2$ at 215 K; this signal results from the overlap of a symmetric signal with $g = 2.138$ (Ni^{2+}) (· · · · · ·) and an asymmetric signal (- - - -) with $g_\perp = 2.06$ and $g_\parallel = 2.35$ (LS Ni^{3+}).

one-component linewidth larger than 30 mT), reproduces well the features of the symmetric experimental spectra observed at $T > T_c$.

This model of dynamic trapping should have detectable consequences on the spin relaxation processes, being directly related to the lifetime of the ion states.

3.4. Temperature dependence of the electron paramagnetic resonance linewidth

The temperature dependence of the EPR linewidth ΔB was previously interpreted as the effect of phonon modulation of dipole–dipole interactions [12]. Nevertheless, the signal narrowing, as well as the asymmetry of the signal appearing just above T_c, may also be related to the lowering of the frequency of the dynamical motion of the hole shared between the nickel ions, down to the complete localization, at T_c, on the Ni^{2+} ions of the 'heavy' layers. In this situation, the asymmetric signal would arise from the overlap of two signals, from Ni^{2+} in elongated octahedra and from LS Ni^{3+} in compressed octahedra (figure 4). The signal-narrowing mechanism, associated with the lowering of the hole hopping frequency by decreasing the temperature to T_c, should prevail over the broadening processes owing to the decrease in the long-wave fluctuations by decreasing the temperature, and to the lower efficiency of the exchange mechanisms with increasing x. This is just what happens in magnetic materials diluted by non-magnetic ions [17] because, when the exchange paths are cut off at random, the spin correlation functions decay more slowly and the exchange narrowing of the EPR line becomes less efficient. Furthermore, by increasing x, T_c is lowered and the hole localization process proceeds in a wide temperature range. The thermal dependence of the linewidth on the lithium content [1, 12] may indeed support this picture (table 1).

3.5. Magnetic interactions

Let us now consider the possible 'magnetic' interactions in the [(Ni^{2+}–O–Ni^{2+})–h^+] complex. In figure 5 we schematize the exchange interactions via oxygen between the nickel

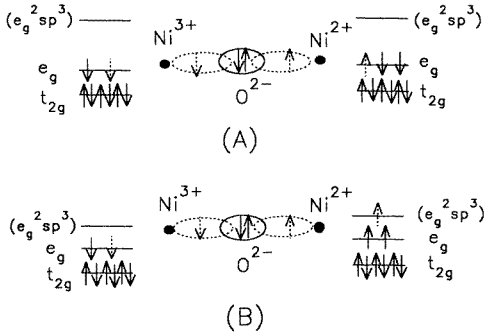

Figure 5. Magnetic interactions in Ni–O–Ni complexes: (A) ferromagnetic interaction between Ni^{3+} and Ni^{2+} ions from the superexchange model; (B) AF interaction resulting from a semicovalent approach. The broken arrows represent the spin excited states.

ions. By following the Anderson [18] approach [19], taking into account only the d orbitals, the system should give rise to ferromagnetic interaction (figure 5(A)). AF interactions may instead be expected if the conditions of the semicovalence model of Goodenough and Loeb [20] and Goodenough [21, 22] are satisfied. This model provides an exchange mechanism mediated by anion–cation bonds which are not strictly covalent, being formed by full anionic orbitals and empty cationic hybrid orbitals. Cationic hybridization may result from d orbitals with non-negligible contributions from the empty s and p cationic orbitals. In this case, a strong overlap may be achieved between full anionic and empty cationic orbitals, allowing the anionic electron with spin parallel to the net cationic spin to spend some of its time in the cationic hybrid orbital.

In our case, according to the proposed local structure, at $T \leqslant T_c$ the Ni^{3+} ions in the LS configuration are localized in the 'heavy' layers, surrounded by compressed octahedra. The upper empty $|3z^2 - r^2\rangle$ orbital allows the creation of a σ-bonding orbital occupied by an anionic electron with spin parallel to the net spin of the Ni^{3+} ion. On the other side of the bridging oxygen, the Ni^{2+} ion is surrounded by an elongated octahedron with the Ni^{2+}–O bond longer than the Ni^{3+}–O bond. In this case, efficient overlap with the oxygen orbitals may be achieved by more extended cationic orbitals such as the hybrid $e_g^2 sp^3$. This situation would match the typical semicovalent model allowing exchange AF interactions (figure 5(B)), if the hybrid orbital is slightly different in energy with respect to the partially filled d levels.

Accounting for AF interactions, our approach agrees with the magnetic properties of these materials [1], confirming that the AF character of the Ni–O–Ni complexes pertains to both Ni^{2+}–O–Ni^{2+} and Ni^{2+}–O–Ni^{3+}, as suggested by Goodenough *et al* [2] if Ni^{3+} is in the LS state.

4. Concluding remarks

The model of hole localization in Ni–O–Ni complexes may be useful to clarify some other particular aspects regarding the transport properties and the magnetic ordering of these materials.

Concerning the conductivity features, it was found that the activation energies of the holes in the electric conduction process are the same in the OSS compound with $x = 0.465$ [15] and in the SSS phase [23]. However, the resistivity of the OSS compound (30 Ω cm)

[15] is an order of magnitude higher than that of the SSS compound with $x = 0.10$ [23], indicating a decrease in the charge carrier density. The lower density of free holes in OSS compounds with respect to SSS phases, despite the larger hole concentration due to the higher lithium content, supports the existence of two distinct types of hole localization: one in shallow traps belonging to stoichiometric regions characterized by the predominance of the Ni–O–Li sequence; the other in much deeper Ni–O–Ni traps like the proposed paramagnetic complexes. So, the trapping in Ni–O–Ni sites should be regarded as competitive with the conduction process. On the other hand, the decrease in Ni–O–Ni sites on approaching the $LiNiO_2$ composition should cause a resistivity lowering, as really observed in nearly stoichiometric compounds showing resistivity values of about 1 Ω cm with the same activation energy [15].

Let us now consider the interpretations of the magnetic properties of the quasi-stoichiometric $LiNiO_2$ samples. In these cases, a few approaches were reported calling for two-dimensional Ising systems (both AF and ferromagnetic [6, 7, 13]) or for Kosterlitz–Thouless transitions of Ising systems [8]. However, the Ising model does not agree with the EPR data, since the spectrum is consistent with a nearly isotropic spin system. Rather, we suggest that the magnetic behaviour of these compounds may arise from the extreme dilution of the Ni–O–Ni complexes responsible for the inter-plane AF order. This is confirmed by very recent magnetic data [7], also indicating the lack of magnetic order by approaching the stoichiometric $LiNiO_2$ compound.

We finally remark that the clustering effects of the Ni–O–Ni complexes may create a variety of regions with different magnetic features; inhomogeneity-induced behaviours were indeed evidenced [24]. In support of this, the EPR signal below T_c shows different components with thermal behaviours varying from sample to sample, probably because of lattice regions with different local fields created by the random distribution of the Ni–O–Ni complexes.

Acknowledgments

The authors gratefully acknowledge Professor A Rigamonti for his interesting and helpful discussions and Dr M C Mozzati for the assistance with measurements and calculations.

References

[1] Azzoni C B, Paleari A, Massarotti V, Bini M and Capsoni D 1996 *Phys. Rev.* B **53** 703
[2] Goodenough J B, Wickham D G and Kroft W J 1958 *J. Phys. Chem. Solids* **5** 107
[3] Corti M, Marini S, Rigamonti A, Massarotti V and Capsoni D 1996 *J. Appl. Phys.* **79**
[4] Massarotti V, Capsoni D and Bini M 1995 *Z. Naturf.* a **50** 155
[5] Ganguly P, Ramaswamy V, Mulla I S, Shinde R F, Bakare P P, Ganapathy S, Rajamohanan P R and Prakash N V K 1992 *Phys. Rev.* B **46** 11 595
[6] Kemp J P, Cox P A and Hodby J W 1990 *J. Phys.: Condens. Matter* **2** 6699
[7] Rougier A, Delmas C and Chouteau G 1996 *J. Phys. Chem. Solids* at press
[8] Stoyanova R, Zhecheva E and Angelov S 1993 *Solid State Ion.* **59** 17
[9] Kuiper P, Kruizinga G, Ghijsen J, Sawatzky G A and Verweij H 1989 *Phys. Rev. Lett.* **62** 221
[10] van Veenendaal M A and Sawatzky G A 1994 *Phys. Rev.* B **50** 11 326
[11] Stoyanova R, Zhecheva E and Friebel C 1993 *J. Phys. Chem. Solids* **54** 9
[12] Stoyanova R, Zhecheva E and Friebel C 1994 *Solid State Ion.* **73** 1
[13] Yamada I, Ubukoshi K and Hirakawa K 1985 *J. Phys. Soc. Japan* **54** 3571
[14] Hirota K, Nakazawa Y and Ishikawa M 1991 *J. Phys.: Condens. Matter* **3** 4721
[15] Kanno R, Kubo H, Kawamoto Y, Kamiyama T, Izumi F, Takeda Y and Takano M 1994 *J. Solid State Chem.* **110** 216

[16] Abragam A and Bleaney B 1970 *Electron Paramagnetic Resonance of Transition Ions* (Oxford: Clarendon) pp 449–55
[17] Benner H and Boucher J P 1990 *Magnetic Properties of Layered Transition Metal Compounds* ed L J DeJongh (Deventer: Kluwer Academic) pp 324–78
[18] Anderson P W 1950 *Phys. Rev.* **79** 350; 1959 *Phys. Rev.* **115** 2
[19] Eskes H and Jefferson J H 1993 *Phys. Rev.* B **48** 9788
[20] Goodenough J B and Loeb A L 1955 *Phys. Rev.* **98** 391
[21] Goodenough J B 1955 *Phys. Rev.* **100** 564
[22] Goodenough J B 1958 *J. Phys. Chem. Solids* **6** 287
[23] Heikes R R and Johnston W D 1952 *J. Chem. Phys.* **26** 582
[24] Reimers J N, Dahn J R, Greedan J E, Stager C V, Liu G, Davidson I and Von Sacken U 1993 *J. Solid State Chem.* **102** 542